Microbes and Infection
Vol. 8, Issues 12-13 , October 2006, P. 2715-2724
http://dx.doi.org/10.1016/j.micinf.2006.07.020

Cellular and molecular hemocyte responses of the Pacific oyster, Crassostrea gigas, following bacterial infection with Vibrio aestuarianus strain 01/32

Yannick Labreuche[a], Christophe Lambert[b], Philippe Soudant[b,*], Viviane Boulo[c], Arnaud Huvet[a] and Jean-Louis Nicolas[a]

[a]Unité Mixte de Recherche Physiologie et Ecophysiologie des Mollusques Marins (UMR 100), IFREMER, Centre de Brest, B.P. 70, 29280 Plouzané, France
[b]Laboratoire des Sciences de l'Environnement Marin, Institut Universitaire Européen de la Mer, Université de Bretagne Occidentale, place Copernic, Technopôle Brest-Iroise, 29280 Plouzané, France
[c]Génome, Populations, Interactions, Adaptation (GPIA), UMR 5171 (IFREMER, CNRS, UMII), Université de Montpellier II, place Eugène Bataillon, CC 80, 34095 Montpellier, France

*: Corresponding author : mailto:philippe.soudant@univ-brest.fr

Abstract:

The strategies used by bacterial pathogens to circumvent host defense mechanisms remain largely undefined in bivalve molluscs. In this study, we investigated experimentally the interactions between the Pacific oyster (Crassostrea gigas) immune system and Vibrio aestuarianus strain 01/32, a pathogenic bacterium originally isolated from moribund oysters. First, an antibiotic-resistant V. aestuarianus strain was used to demonstrate that only a limited number of bacterial cells was detected in the host circulatory system, suggesting that the bacteria may localize in some organs. Second, we examined the host defense responses to V. aestuarianus at the cellular and molecular levels, using flow-cytometry and real-time PCR techniques. We showed that hemocyte phagocytosis and adhesive capabilities were affected during the course of infection. Our results also uncovered a previously-undescribed mechanism used by a Vibrio in the initial stages of host interaction: deregulation of the hemocyte oxidative metabolism by enhancing the production of reactive oxygen species and down-regulating superoxide dismutase (Cg-EcSOD) gene expression. This deregulation may provide an opportunity to the pathogen by impairing hemocyte functions and survival. These findings provide new insights into the cellular and molecular bases of the host–pathogen interactions in C. gigas oyster.

Keywords: Bivalve immunity; Vibrio aestuarianus; Pathogenesis; Oyster; Crassostrea gigas

1. Introduction

The interaction between microorganisms and host immune defenses is a key determinant in the outcome of disease processes. Partly as a result of the simple and conserved mechanisms constituting their innate immune systems, invertebrates have become a paradigm for the study of bacterial virulence and the characterization of host-pathogen interactions. Several invertebrate groups, including nematodes [1] and insects [2], have been investigated extensively, providing important insights into how these animals recognize and defend themselves against infectious agents. In comparison, little is known about bivalve-bacteria interactions and associated immune responses. As filter feeders, bivalves are exposed to a constant challenge by various pathogenic and/or opportunistic bacteria naturally present in the microflora of coastal environments. Although lacking an adaptive immune system, these animals have evolved an effective mechanism for clearing invading bacteria, based upon a complex interplay between cellular and humoral defense responses. The cellular immune system relies specifically on immuno-competent cells, referred to collectively as hemocytes. In some bivalves, three major hemocyte types are commonly recognized: granulocytes, hyalinocytes and agranulocytes. These cells are responsible for activities such as inflammation, wound repair, phagocytosis and encapsulation of non-self particles [3]. The hemolymph (circulating, extracellular fluid) also contains humoral immune components, including antimicrobial peptides [4], agglutinins [5] and lysosomal enzymes [6]. These components enhance opsonization by facilitating bacterial aggregation and immobilization, and/or display cytolytic activities. Bacterial clearance from hemolymph and tissues results, thus, from the combined action of humoral defense factors and the hemocyte phagocytic process.

However, some bacteria, mainly belonging to the *Vibrio* genus, are able to persist within bivalve tissues and fluids [7]. Many pathogenic bacteria have developed sophisticated strategies to circumvent host defense mechanisms, thereby finding unique niches where they can survive, and from which they can establish successful infection. For example, *V. tapetis*, the causative agent of brown ring disease in the clam *Ruditapes philippinarum* [8], elicits major changes in hemocyte morphology and escapes phagocytosis by impairing hemocyte adhesion properties [9, 10].

Reported as commensal bacteria, vibrios are also considered to be opportunistic pathogens. They can be associated with mortalities of bivalves, particularly Pacific oysters, *Crassostrea gigas* [11]. Recently, a *V. aestuarianus* strain, named 01/32, was isolated during a mortality outbreak in an experimental hatchery; its pathogenicity was assessed by experimental challenge, resulting in high *C. gigas* mortality rates [12]. In an earlier study, we showed that its extracellular products (ECPs) displayed lethality to animals and induced, *in vitro*, a strong inhibition of hemocyte phagocytosis and adhesive abilities [13]. These results suggest that the production of ECPs by the pathogen plays an important role in the pathological processes.

Many questions remain unanswered concerning the *in vivo* interaction between *V. aestuarianus* and the oyster immune responses. First, little is known about bacterial colonization within the oyster following introduction of *V. aestuarianus* within the circulatory system. This is mainly because it is difficult to quantify selectively one bacterium among the indigenous microflora of oyster hemolymph, which is sometimes composed of numerous bacterial species [14]. Second, the different phases of infection (i.e. from the initial host-pathogen interaction to the activation of the host immune responses) remain poorly understood. Previous *in vivo* studies in bivalves have examined the host responses to invading

pathogens either at the cellular [15-17] or at the molecular level [18, 19], but neither considering both. In such a context, monitoring the host immune system with a global approach may contribute to gain an insight into the strategies evolved by *V. aestuarianus* 01/32 to impair immunity and survival of *C. gigas* oysters.

These experiments were designed, therefore, to document during an experimental infection the number of recoverable *V. aestuarianus* 01/32 within oyster hemolymph. To do so, we used an antibiotic-resistant *V. aestuarianus* mutant and further investigated its effects i) on oyster cellular immune defenses by performing flow cytometric-based hemocyte assays, and ii) on host molecular immune responses using real-time PCR techniques.

2. Materials and methods

2.1 Oysters

Two-year-old Pacific oysters, *Crassostrea gigas* (8-13 cm in shell length), were provided by a French commercial hatchery (Aber-Benoît, Finistère, France). Animals were acclimated for one week in the laboratory (IFREMER, Plouzané, France), as previously described [13].

2.2 Selection of a spontaneous *V. aestuarianus* 01/32 mutant with decreased susceptibility to kanamycin

V. aestuarianus strain 01/32 was grown overnight in antibiotic-free Marine Broth (MB, Difco) (20°C, 20 h, shaker table at 200 rpm), harvested by centrifugation (1500 G, 10 min) and resuspended in filtered (0.22 µm) sterile seawater (FSSW) to obtain an inoculum of 10^9 cfu.ml^{-1}. Marine Agar (MA, Difco) plates containing kanamycin (Sigma) at a concentration of 100 µg.ml^{-1} were inoculated with 100 µl of the bacterial suspension and incubated at 20°C for 24 h. One colony with the typical size and morphology of the original strain was randomly chosen from selecting plates and sub-cultured onto MA containing kanamycin (100 µg.ml^{-1}). This spontaneous mutant was compared with the wild-type strain by phenotypic and genotypic characterization. Results were found to be identical for the two strains (data not shown). For a subsequent infection experiment, the antibiotic-resistant *V. aestuarianus* 01/32 was grown overnight in kanamycin-appended MB. Following incubation, bacterial cells were prepared as described previously [13].

2.3 Experimental infection

To facilitate delivery of the inoculum, a small notch was carved in the dorsal side of the oyster shell, adjacent to the adductor muscle. After filing the shell, animals were acclimated for 5 days. Oysters were subsequently challenged by injecting either 100 µl of FSSW or 100 µl of the kanamycin-resistant *V. aestuarianus* 01/32 suspension ($5x10^7$ cfu per oyster) into the adductor muscle. Two-hundred forty oysters (4 replicate tanks, 60 oysters per tank) were injected with kanamycin-resistant *V. aestuarianus* 01/32 (vibrio-inj), 240 (4 replicate tanks, 60 oysters per tank) with FSSW (fssw-inj) and a further 240 (4 replicate tanks, 60 oysters per tank) were not injected (non-inj). After handling, animals were returned to seawater tanks maintained under static conditions.

The problem we faced was to determine the oyster cumulative mortality rates during the course of infection, since 4 to 5 animals from each tank were planned to be removed every 2 days for hemolymph sampling. Accordingly, at the beginning of the experiment, 10 oysters were randomly selected and marked in each replicate tank. These animals were only used to record mortalities and were thus not collected for hemolymph bleeding. Animals were considered to be dead when the valves did not close and the mantle did not react after stimulation by a needle-prick.

2.4 Hemolymph sampling

Hemolymph samples were collected 1, 3, 5 and 8 days post-challenge. Samples were aseptically withdrawn from the adductor muscle using a 1-ml plastic syringe fitted with a 25-gauge needle, and stored individually in micro-tubes held on ice, to minimize cell clumping. Individual samples were observed under the optical microscope to control the quality of the

hemolymph used subsequently, and to prevent gamete contamination. Hemolymph was then filtered through 80-µm mesh. One hemolymph pool, comprised of 4-5 individual samples, was prepared for each tank. Each pool was aliquoted into 3 volumes: one aliquot was used for quantifying the number of bacterial cells and evaluating the hemolymph protease activity, another was used for measuring the immunological parameters by flow cytometry, and the last for analyzing gene expression by real-time PCR.

2.5 Direct quantification of kanamycin-resistant *V. aestuarianus* 01/32

To quantify the number of recoverable kanamycin-resistant *V. aestuarianus* 01/32 cells within oyster hemolymph, a dye reduction-based method was applied. This assay was adapted from the method of Volety *et al.* [20] and used a tetrazolium compound, MTS [3-(4,5-dimethylthiazol-2-yl)-5-(3-carboxymethoxphenyl)-2-(4-sulfophenyl)-2H-tetrazolium], as a substrate, which in the presence of PMS [phenazine methosulfate] is reduced by living bacterial cells in proportion to their numbers. MTS and PMS reagents were obtained from Promega (Madison, USA) and prepared as previously described [20]. After bleeding, 150 µl sub-samples from each hemolymph pool were centrifuged for 15 min at 200 G to precipitate hemocytes. For each pool, triplicate aliquots (25 µl) of cell-free serum, or hemocyte pellet resuspended in FSSW (25 µl), were spread on 96 well microtiter plates. Three wells were processed in each plate with FSSW as a control. A recovery-growout period for surviving kanamycin-resistant *V. aestuarianus* 01/32 cells was then started by adding kanamycin-appended MB (100 µl), and incubating at 18°C for 24 h. MTS/PMS (20 µl) was added in each well and incubation was continued for an additional 30 min at room temperature. Finally, measurements of formazan (the reduction product of MTS/PMS) were performed colorimetrically at 492 nm. Bacterial cell numbers were determined using a previously

established relationship, according to the procedure of Volety *et al.* [20]. To estimate the total bacterial load within cell-free serum samples, the reduced MTS/PMS absorbance was finally evaluated for each experimental condition by performing the assay without adding the antibiotic solution to the reaction mixture.

2.6 Determination of hemolymph protease activity

V. aestuarianus strain 01/32 was previously shown to produce extracellular products (ECPs), lethal to *C. gigas* oysters [13]. Two methods were therefore applied to monitor the production of ECPs by *V. aestuarianus* 01/32 in oyster hemolymph. Total protease activity was measured by the azocasein procedure [21], and one unit of protease activity was expressed as an increase in absorbance at 440 nm of 1 for 10 min of incubation at 20°C. Electrophoretic protease patterns were assessed by zymographic procedures [22].

2.7 Hemocyte cellular parameters

Measurements of hemocyte types, numbers, and functions were performed on a FACScalibur flow cytometer (Becton-Dickinson, San Diego, CA, USA), equipped with a 488 nm argon laser.

2.7.1 Total hemocyte count (THC)

Briefly, a 100 µl sub-sample of each hemolymph pool was diluted with 200 µl anti-aggregant solution (AASH) and 100 µl FSSW. Samples were then incubated at 18°C for 120 min with SYBR Green I (1% final concentration), a DNA-binding fluorochrome which stains hemocyte DNA (Molecular Probes, USA). Hemocyte concentration was determined by

using a density plot visualization of FL1 *vs* SSC (Side SCatter height) to count hemocytes that had been detected by the flow-cytometer for defined time and flow rate.

2.7.2 Phagocytosis of fluorescent beads

The phagocytosis assay was adapted from the method of Delaporte *et al.* [23], using fluorescent latex beads (Fluoresbrite, YG Microspheres, 2 µm, Polysciences). A 150 µl sub-sample of each hemolymph pool was distributed into a 5 ml polystyrene tube (Falcon, B-D Biosciences, San Jose, CA, USA), diluted (+ 150 µl) with FSSW and maintained on ice. Each sub-sample was subsequently combined with 30 µl of fluorescent bead working solution (2% of the commercial solution in FSSW, final concentration $1x10^7$ beads.ml^{-1}) and incubated at 18°C for 120 min. Tubes were then analyzed on the flow cytometer. Results were expressed as the percentage of hemocytes containing three beads or more [13].

2.7.3 Adhesive capacity

To estimate hemocyte adhesive capacity, sub-samples (100 µl) of each hemolymph pool were distributed into 24-well microplates maintained on ice. Each sub-sample received a 100 µl volume of FSSW. After three hours of incubation at 18°C, cells were fixed by addition of 200 µl of a 6% formalin solution in FSSW. Concentration of non-adherent cells was established as previously described [13]. The percentage of adhering hemocytes was calculated relatively to the initial total hemocyte count of the tested pool.

2.7.4 Reactive oxygen species (ROS) production

The method used 2'7'-dichlorofluorescein diacetate (DCFH-DA, Sigma) [24]. Briefly, a 150 µl sub-sample of hemolymph from each pool was distributed into a 5 ml polystyrene tube (Falcon, B-D Biosciences, San Jose, CA, USA), diluted (+ 150 µl) with FSSW and

maintained on ice. DCFH-DA working solution was added to each tube to yield a final concentration of 10 µM. Tubes were then incubated for 60 min at 18°C in the dark. The DCF green fluorescence level was evaluated for the three hemocyte sub-populations (agranulocytes, hyalinocytes and granulocytes), as described previously [13]. Small agranulocytes showing very low ROS production, values for hyalinocytes and granulocytes only are presented here. Results are given for both hemocyte sub-populations as mean of fluorescence in FL1 arbitrary units.

2.8 Real-time PCR analysis of gene expression

Hemocytes were pelleted by centrifugation (1800 G, 15 min) and resuspended in Extract-All® (Eurobio) (1 ml.10^{-7} cells) to extract total RNAs. Total RNA samples were first treated with 2 U DNase I Amplification Grade (Invitrogen) to remove contaminating genomic DNA. Total isolated RNAs (1.5 µg) were subsequently reverse-transcribed in a final volume of 20 µl using 1 µl oligo$(dT)_{12\text{-}18}$ (0.5 µg.μl^{-1}) and 200 U MMLV reverse transcriptase (Invitrogen) according to the supplier's instructions. As non-inj and fssw-inj oysters showed no statistical differences in any of the tested cellular parameters (see sections 3.4 to 3.7), real-time PCR analysis was performed only on vibrio-inj and fssw-inj animals. The relative expression of the tissue inhibitor of metalloproteinases (*Cg-TIMP*) and the extracellular superoxide dismutase (*Cg-EcSOD*) was investigated by real-time PCR, using a LightCycler® Instrument (Roche). Amplification of oyster *Elongation Factor I* (*EF*) cDNA (GenBank AB 122066) was performed to confirm the steady-state expression of a housekeeping gene, allowing an internal control for *Cg-EcSOD* and *Cg-TIMP* gene expression. *Cg-TIMP* and *Cg-EcSOD* specific primers were TimpF (5'-TGAGGCAGTACAACTTCCTTCTATT-3'), TimpR (5'-ACCCCTTGAATATGTCTCTCTTCTT-3') (C. Montagnani, unpublished), and

SodF (5'-ACGGACTTCAGATCCACGAG-3'), SodR (5'-GGCCAAGAATTCCGTCTGTA-3') (M. Gonzales, unpublished), respectively. *EF* primers were those used by Montagnani *et al.* [25]. PCR reactions were set up according to the LightCycler system version 3.5, with 0.5 µM of each primer and 2 µl Lightcycler Fast Start DNA Master SYBR Green I (Roche Molecular Biochemicals), in a total volume of 9.5 µl. The mix was thereafter introduced into the LightCycler glass capillaries, and 0.5 µl cDNA was added as the PCR template. The real-time PCR assay consisted of an initial denaturation step at 95°C for 10 min, amplification and quantification programs repeated 40 times (94°C for 15 s, annealing temperature: at 62°C (*EF, Cg-TIMP*), 60°C (*Cg-EcSOD*) for 5 s and extension at 72°C for 10 s) and a melting curve program (65 to 95°C with a heating rate of 0.05°C/s). For each reaction, the crossing point (CP) was determined using the "Fit Point Method" of the LightCycler Software 3.5. Each run included a blank control (H_2O control) and a positive cDNA control (plasmid with the corresponding gene ORF as template). The PCR efficiency (E) was calculated by the standard curve method: $E = 10^{(-1/slope)}$ [26]; this value was determined for each primer pair by performing standard curves from serial dilutions of each positive cDNA control to ensure that E ranged from 99% to 100%.

Calculated relative expression was based on the "comparative CP method" [27]. The overall variation in *EF* expression was determined using two-way analysis of variance to test for differences in mean CP value between all the experimental groups. No significant ($P>0.05$) interaction between the two main factors (i.e time and condition) was shown, confirming the consistent expression of *EF* between the two experimental groups within each time point. The fold change in the target gene, normalized to *EF* and relative to the expression at time zero, was expressed for each sample as $2^{-\Delta\Delta Ct}$ [27], where :

$$\Delta\Delta Ct = [(Ct_{Target} - Ct_{EF})_{Time\ x} - (Ct_{Target} - Ct_{EF})_{Time\ 0}].$$

2.9 Statistical analysis

Significant differences between treatments during each assay were tested by one-way analysis of variance (ANOVA) or the Kruskal-Wallis test in case of heterogeneity of variances, using Statgraphics Plus 5.0 software. Data collected as percentages were transformed (arcsin of the square root) before analysis but are presented in figures as untransformed percentage values. The method used to discriminate among the means was Fisher's least significant difference (LSD) procedure. Results were deemed significant at $P<0.05$.

3. Results

3.1 Bacterial challenge

Cumulative mortality data of non-inj and fssw-inj oysters demonstrated no significant differences over the experiment (ANOVA, $P>0.05$) (Fig. 1). Compared to the other experimental conditions, mortality rates of vibrio-inj animals were statistically higher at day 3 post-challenge, and significantly increased over time, to reach 62.5 ± 1.2 % at the end of the experiment (ANOVA, $P<0.05$).

3.2 Direct quantification of kanamycin-resistant *V. aestuarianus* 01/32

In cell-free serum samples of non-inj and fssw-inj oysters, no kanamycin-resistant bacteria were detected throughout the experimental period (data not shown). At 1 day post-challenge, a concentration of $3.2x10^2 \pm 1\times10^2$ cells.ml^{-1} was determined in cell-free serum of vibrio-inj oysters (Fig. 2 A). After 3 days, this number decreased to reach a concentration close to 10^2 cells.ml^{-1}, corresponding to the threshold of sensitivity for this method, and remained low and stable over the experiment.

In hemocyte pellet samples of vibrio-inj animals, a bacterial concentration lower than the threshold of sensitivity of the MTS/PMS assay was found the last day of the experiment, whereas no kanamycin-resistant bacteria were detected for the other experimental conditions (data not shown). The total bacterial load within cell-free serum samples was also estimated by measuring the reduced MTS/PMS absorbance without adding the antibiotic to the reaction mixture. For the 3 experimental conditions, no significant differences were observed at 3 and 5 days post-challenge (ANOVA, $P>0.05$) (Fig. 2 B). At the end of the experiment, absorbance

values of vibrio-inj oysters were statistically higher compared to control animals (ANOVA, $P<0.05$).

3.3 Hemolymph protease activity

Azocasein-based assays showed no statistical differences in hemolymph protease activity between non-inj and fssw-inj animals throughout the experiment (ANOVA, $P>0.05$) (Fig. 3 A). Three days post-challenge, a significant rise occurred in hemolymph protease activity of vibrio-inj oysters, compared to day 1 and to the other experimental conditions. Subsequently, hemolymph protease activity of vibrio-inj animals increased steadily and significantly over the experiment (Fig. 3 A).

The patterns of gelatinolytic activity in hemolymph pools of fssw-inj oysters were similar to those observed for non-inj animals (data not shown). For these two conditions, bands with protease activity in the 123 kDa range were detectable throughout the experimental period (Fig. 3 B). Within the first 3 days following injection, similar protease profiles were observed in hemolymph samples of vibrio-inj oysters. However, important modifications occurred on day 5: the 123 kDa bands were missing from hemolymph of vibrio-inj animals, whereas two additional bands with a molecular weight lower than 80 kDa, as well as a faint band with a low molecular weight, were detected. These three bands were most prevalent 8 days post-challenge and were similar to the protease profiles resulting from the zymographic detection of extracellular products from *V. aestuarianus* 01/32 in pure culture, as shown in Fig. 3 B.

3.4 Total number of circulating hemocytes

Non-inj and fssw-inj oysters showed no statistical difference in their total hemocyte counts (THC) throughout the experiment (ANOVA, $P>0.05$) (Fig. 4). In vibrio-inj animals, a significant increase of THC values (+ 91%) was observed 3 days post-infection, compared to non-inj and fssw-inj oysters (ANOVA, $P<0.05$). Five days post-challenge, THC of infected-oysters remained significantly higher than non-inj and fssw-inj animals. The last day of the experiment, THC values of vibrio-inj animals returned to levels similar to those observed for non-inj and fssw-inj oysters (ANOVA, $P>0.05$).

3.5 Hemocyte phagocytic activity

One and 3 days post-challenge, no statistical difference in hemocyte phagocytic activity was observed between experimental conditions (ANOVA, $P>0.05$) (Fig. 5). In vibrio-inj animals, the phagocytic activity statistically decreased on day 8 post-challenge, compared to control animals (ANOVA, $P<0.05$).

3.6 Hemocyte adhesive capacity

Non-inj and fssw-inj oysters were not statistically different in their adhesive capacities for the entire experiment (ANOVA, $P>0.05$) (Fig. 6). By contrast, hemocyte capacity for adhesion of vibrio-inj oysters was significantly reduced after one day post-challenge, compared to non-inj and fssw-inj oysters (ANOVA, $P<0.05$) (Fig. 6). Afterwards, hemocyte adhesive ability of infected animals decreased significantly and regularly (ANOVA, $P<0.05$).

3.7 Hemocyte ROS production

ROS production remained stable over the experimental period in non-inj and fssw-inj oysters for the two hemocyte sub-populations (Fig. 7). In contrast, granulocyte ROS production of vibrio-inj animals was enhanced from day 3, and was significantly higher than those of non-inj and fssw-inj oysters (ANOVA, $P<0.05$) (Fig 7 A). Considering hyalinocyte sub-populations, a similar pattern was observed, except that the ROS production of hyalinocytes from vibrio-inj oysters was lower than that observed for granulocytes (Fig. 7 B).

3.8 Relative mRNA levels of *Cg-TIMP* and *Cg-EcSOD*

Cg-EcSOD mRNA level (relative to *EF* mRNA) remained stable in fssw-inj oysters over the course of the experiment (ANOVA, $P>0.05$) (Fig. 8 A). In contrast, the level of *Cg-EcSOD* mRNA expression in vibrio-inj animals decreased significantly by 3.6 fold on day 1 ($P<0.05$) and by 8.3 fold on day 3 ($P<0.05$), compared to fssw-inj oysters. Following this initial decrease, the relative level of *Cg-EcSOD* transcripts increased in vibrio-inj animals after 5 days, to reach similar values as those observed in fssw-inj oysters (ANOVA, $P>0.05$).

Cg-TIMP relative expression remained stable for the duration of the experiment for both vibrio-inj and fssw-inj animals (Fig. 8 B). No significant differences were shown between these two experimental groups at each sampling date (ANOVA, $P>0.05$).

4. Discussion

This work was aimed at investigating oyster cellular immune responses following injection of a pathogenic *Vibrio* into the adductor muscle. Other less invasive methods of infection have been previously tested in marine molluscs, and successful reproduction of disease or mortalities were obtained in larval challenge by bathing (see [28] for a review). However, cohabitation or bacterial bath exposures are more problematic to conduct experiments in juvenile and adult molluscs, since they often fail to induce any mortality or led to unreproducible results [29-31]. Such difficulties to perform non invasive bacterial challenges in adult bivalves are suspected to be linked with the need for external stressors [32, 33] and/or with the variability of the bivalve physiological and health status [34, 35]. Intramuscular injection of bacteria was consequently considered as the most suitable mode of inoculation to address the questions of this study and also to insure a better reproducibility.

4.1 Following *V. aestuarianus* 01/32 injection into the oyster adductor muscle, bacteria do not spread within the host circulatory system

In this experimental model, we showed that a low bacterial load of kanamycin-resistant *V. aestuarianus* 01/32 was detected in cell-free serum of infected oysters. This was an unexpected result, since the pathogen was previously isolated, at high concentrations in some cases, from the hemolymph of moribund animals [12]. As this result might be ascribed to the phagocytic uptake of bacteria by hemocytes, complementary experiments were performed over the experiment. A low bacterial concentration ($< 10^2$ cells.ml^{-1}) was determined within hemocytes of infected animals, indicating that the proportion of engulfed bacteria was limited and did not account for the drop of *V. aestuarianus* cell number. The reduced number of kanamycin-resistant *V. aestuarianus* in hemolymph could also be

explained by a loss of the antibiotic resistance. In such case, an increase in total bacterial concentration of infected animals would have been expected. However, when the bacterial flora of cell-free serum samples was estimated in non-selective conditions, no significant changes in MTS/PMS absorbance (related to the bacterial concentration) were observed for the 3 experimental conditions at 3 and 5 days post-challenge, invalidating this hypothesis. At the end of the experiment, the increase in absorbance of infected oysters, although statistically significant, remained quite restrained. Overall, data obtained here suggest that the pathogen may have localized in some organs or tissues during infection, from which ECPs were released. Histological observations of oysters infected by *V. aestuarianus* 01/32 under the same experimental conditions support this assumption. Bacteria were indeed localized in foci between muscular fibers of the adductor muscle, whereas no bacterial aggregates were observed in the other organs or tissues (unpublished results).

Whether this infection remains localized or proceeds into surrounding tissues partly depends upon the pathogen's capacity to disrupt the components of the host connective tissues, among which the extracellular matrix (ECM) that holds tissues together [36]. Under normal physiological conditions, ECM degradation is tightly controlled by endogenous inhibitors, called tissue inhibitors of metalloproteinases (TIMPs). Considering that the pathogen may induce necrotic reactions of ECM, we monitored *Cg-TIMP* relative expression. Following bacterial challenge, previous report showed that *Cg-TIMP* mRNAs strongly accumulated in *C. gigas* hemocytes, reaching a maximum around 9 h post-infection and returning to a steady state after 3-4 days [18]. In our experimental model, no significant changes occurred in *Cg-TIMP* relative expression of infected oysters. This discrepancy may be due to the bacterial species used, as Montagnani *et al.* injected a mixture of four different vibrios. *V. aestuarianus* 01/32 may thus act according to a different mechanism. These data correlate well with bacterial quantification results and suggest that the pathogen may not

induce connective tissue damage through ECM degradation, and thus may not spread within the host. To assess this hypothesis, specific molecular tools are currently being developed for further histopathological studies.

4.2 Infection induces important changes in the total number of circulating hemocytes

Hemocyte recruitment is one of the first cellular responses of the host defense system against pathogens [3]. Variations in hemocyte concentration were therefore monitored during infection. In infected animals, a transient increase in circulating hemocytes was observed within the first 3 days post-challenge. Such variations in cell concentration may result either from hemocyte mobilization from tissues into the circulatory system, or from a hematopoietic process that would change the absolute number of circulating hemocytes. Following microbial challenges, similar observations were previously reported in bivalves [15, 16]. The most generally-accepted belief is that the elevated cell concentration result from a mobilization and migration of resident hemocytes from tissues into the hemolymph in response to host-pathogen interactions [15-17]. This phenomenon, also called hemocytosis, is suspected to be linked with the structure of the circulatory compartment in bivalves and would correspond to a non-specific immune response. Further investigations are needed to clarify which of these mechanisms (i.e. hematopoiesis vs. hemocytosis) is involved in the noticed changes.

4.3 The pathogen may evade host cellular defenses by inhibiting hemocyte adhesive and phagocytic capacities

Adhesion constitutes an initial step in phagocytosis of foreign particles and results in important cellular behaviors, such as microbe encapsulation. In this study, we showed that adhesive capabilities of circulating hemocyte were significantly affected from the first day

post-infection. Hemocyte phagocytosis capacities were also reduced, but the decrease of phagocytic activities occurred later, when the production of bacterial proteases was at its highest level. These results correlate well with our data of bacterial quantification, demonstrating that a limited number of *V. aestuarianus* cells was detected within oyster hemocytes. Taken together, these findings suggest that the pathogen may have evolved a so-called “outsider strategy”, to promote its own extracellular life cycle within the oyster. This assumption is reinforced by our previous *in vitro* studies, showing that *V. aestuarianus* ECPs drastically affected hemocyte functions by causing an inhibition of adhesive and phagocytic activities [13]. Observations of similar effects during infection, concurrent with the secretion of bacterial proteases in hemolymph, lead us to suspect that avoidance of phagocytosis may be attributable to the release in the host circulatory system of one or more adhesion- and phagocytosis-inhibiting factors. Research is now ongoing to elucidate the mechanisms by which this pathogen mediates its antiphagocytic phenotype.

4.4 The ROS production pathway is strongly modified during bacterial infection

In the cascade of events taking place during the host immune response, a subsequent step relies on the production of reactive oxygen species (ROS), displaying strong microbicidal activities [37]. We showed that, during infection, hyalinocyte and granulocyte ROS production was strongly enhanced in animals. These data are surprising when compared with previous results obtained in bivalves following bacterial challenge. In most of cases, bacteria were, instead, shown to reduce hemocyte ROS production [24, 38, 39]. Our results suggest that *V. aestuarianus* 01/32 may have evolved a different strategy. An increasing number of studies indeed report data on the ability of pathogenic bacteria to escape host cellular responses through an excessive generation of free radicals [40-42]. This over-activation is thought to enhance the virulence by inducing oxidative stress, loss of cell function, and

ultimately cell apoptosis and/or tissue necrosis. The most straightforward evidence is the induction of cell apoptosis by treatments with ROS themselves [43, 44]. The noticed over-activation of ROS production may similarly promote toxicity to host cells, and hemocytes may be both a source and a target of free radicals. The recent report of Terahara and coworkers supports this assumption, as the authors indicated that *C. gigas* hemocytes underwent apoptosis following exposure to ROS generated by the hemocytes themselves [45]. Under normal physiological conditions, a balance exists between the level of ROS produced during normal cellular metabolism and the level of endogenous antioxidants, whose function is to protect tissues from oxidative damage. Among antioxidant enzymes, superoxide dismutases (SODs) are considered as the first and most important line of defense against ROS [46]. Regarding the strong effect of the pathogen on ROS synthesis, we postulated thus a transcriptional activation of *Cg-EcSOD* during the experiment. It was somewhat surprising to find that *Cg-EcSOD* mRNA levels strongly decreased within the first 3 days post-infection, while ROS production was enhanced. This down-regulation, along with the increased rate of free radicals, may overwhelm the host cell defenses, leading to an oxidative stress that may be involved in the pathogenesis. However, further experiments are needed to investigate this assumption.

This is the first study in bivalves reporting a comprehensive analysis of the oyster immune responses both at cellular and molecular levels. The findings of this experimental model of infection contribute to understand the strategies developed by *V. aestuarianus* 01/32 to impair immunity and survival of *C. gigas* oysters. Research is now ongoing to determine the penetration route of the pathogen in oysters and therefore develop a natural model of infection, which may be useful to further characterize the *in vivo* interactions between *V. aestuarianus* 01/32 and the oyster immune system.

Acknowledgments

The authors are indebted to Dr G. H. Wikfors, NOAA Fisheries, Northeast Fisheries Science Center (Connecticut, USA) for the critical review of the first draft of the manuscript and for his help in editing the English language. We are grateful to Marcello Gonzales, Yannick Gueguen (GPIA UMR 5171, Montpellier, France), Jean Michel Escoubas (EMIP UMR 1133, Montpellier, France) and Caroline Montagnani (IFREMER, Tahiti, French Polynesia) for communicating the real-time PCR primer sequences of *Cg-EcSOD* and *Cg-TIMP* before publication. We sincerely thank Patricia Mirella Da Silva Scardua and Marcos Scardua (LEMAR, IUEM, France) for their technical assistance, as well as Céline Garcia (IFREMER La Tremblade, France) for her expertise and assistance in examining histopathological results. We also gratefully acknowledge the skilful assistance of Philippe Miner, Sylvie Gros and Matthieu Garnier (IFREMER Brest, France). This work was supported by the MOREST national project funded by IFREMER, the Régions Basse-Normandie, Bretagne, Pays de la Loire and Poitou-Charentes and by the Conseil Général du Calvados. Y. Labreuche was supported by a doctoral grant from IFREMER and Région Bretagne. Contribution N°XXX of the IUEM, European Institute for Marine Studies (Brest, France).

References

[1] M. J. Gravato-Nobre, and J. Hodgkin, *Caenorhabditis elegans* as a model for innate immunity to pathogens, *Cell. Microbiol.* **7** (2005) 741-751.

[2] D. A. D'Argenio, L. A. Gallagher, C. A. Berg, and C. Manoil, *Drosophila* as a Model Host for *Pseudomonas aeruginosa* Infection, *J. Bacteriol.* **183** (2001) 1466-1471.

[3] T. C. Cheng, Hemocytes: Forms and functions., The Eastern Oyster *Crassostrea virginica* (V.S. Kennedy, R.I.E. Newell, & A.F. Eble, eds.) Maryland Sea Grant, College Park, MD, USA. (1996) 299-333.

[4] E. Bachere, Y. Gueguen, M. Gonzalez, J. de Lorgeril, J. Garnier, and B. Romestand, Insights into the anti-microbial defense of marine invertebrates: the penaeid shrimps and the oyster *Crassostrea gigas*, *Immunol. Rev.* **198** (2004) 149-168.

[5] J. A. Olafsen, T. C. Fletcher, and P. T. Grant, Agglutinin activity in Pacific oyster (*Crassostrea gigas*) hemolymph following *in vivo Vibrio anguillarum* challenge, *Dev. Comp. Immunol.* **16** (1992) 123-138.

[6] Q.-G. Xue, K. L. Schey, A. K. Volety, F.-L. E. Chu, and J. F. La Peyre, Purification and characterization of lysozyme from plasma of the eastern oyster (*Crassostrea virginica*), *Comp. Biochem. Physiol. B Biochem. Mol. Biol* **139** (2004) 11-25.

[7] R. L. Murphree, and M. L. Tamplin, Uptake and retention of *Vibrio cholerae* O1 in the Eastern oyster, *Crassostrea virginica*, *Appl. Environ. Microbiol.* **61** (1995) 3656-3660.

[8] C. Paillard, P. Maes, and R. Oubella, Brown Ring Disease in clams, *Annu. Rev. Fish Dis.* **4** (1994) 219-240.

[9] G. Choquet, P. Soudant, C. Lambert, J. L. Nicolas, and C. Paillard, Reduction of adhesion properties of *Ruditapes philippinarum* hemocytes exposed to *Vibrio tapetis*, *Dis. Aquat. Organ*. **57** (2003) 109-116.

[10] B. Allam, and S. E. Ford, Effects of the pathogenic *Vibrio tapetis* on defence factors of susceptible and non-susceptible bivalve species: I. Haemocyte changes following *in vitro* challenge, *Fish Shellfish Immunol.* **20** (2006) 374-383.

[11] C. Paillard, F. Le Roux, and J. J. Borrego, Bacterial disease in marine bivalves, a review of recent studies : Trends and evolution, *Aquat. Living Res.* **17** (2004) 477-498.

[12] M. Garnier, Y. Labreuche, C. Garcia, M. Robert, and J. L. Nicolas, Evidence for the involvement of pathogenic bacteria in summer mortalities of the Pacific oyster *Crassostrea gigas*, *Microb. Ecol.* In Press (2006).

[13] Y. Labreuche, P. Soudant, M. Goncalves, C. Lambert, and J. L. Nicolas, Effects of extracellular products from the pathogenic *Vibrio aestuarianus* strain 01/32 on lethality and cellular immune responses of the oyster *Crassostrea gigas*, *Dev. Comp. Immunol.* **30** (2006) 367-379.

[14] R. R. Colwell, and J. Liston, Microbiology of shellfish. Bacteriological study of the natural flora of Pacific oysters (*Crassostrea gigas*), *Appl. Microbiol.* **8** (1960) 104-109.

[15] B. Allam, C. Paillard, M. Auffret, and S. E. Ford, Effects of the pathogenic *Vibrio tapetis* on defence factors of susceptible and non-susceptible bivalve species: II. Cellular and biochemical changes following *in vivo* challenge, *Fish Shellfish Immunol.* **20** (2006) 384-397.

[16] R. Oubella, P. Maes, C. Paillard, and M. Auffret, Experimentally induced variation in hemocyte density for *Ruditapes philippinarum* and *R. decussatus* (Mollusca, Bivalvia), *Dis. Aquat. Organ.* **15** (1993) 193-197.

[17] R. Oubella, P. Maes, B. Allam, C. Paillard, and M. Auffret, Selective induction of hemocytic response in *Ruditapes philippinarum* (Bivalvia) by different species of *Vibrio* (Bacteria), *Aquat. Living Res.* **9** (1996) 137-143.

[18] C. Montagnani, F. Le Roux, F. Berthe, and J.-M. Escoubas, *Cg*-TIMP, an inducible tissue inhibitor of metalloproteinase from the Pacific oyster *Crassostrea gigas* with a potential role in wound healing and defense mechanisms, *FEBS Lett.* **500** (2001) 64-70.

[19] A. Huvet, A. Herpin, L. Degremont, Y. Labreuche, J.-F. Samain, and C. Cunningham, The identification of genes from the oyster *Crassostrea gigas* that are differentially expressed in progeny exhibiting opposed susceptibility to summer mortality, *Gene* **343** (2004) 211-220.

[20] A. K. Volety, L. M. Oliver, F. J. Genthner, and W. S. Fisher, A rapid tetrazolium dye reduction assay to assess the bactericidal activity of oyster (*Crassostrea virginica*) hemocytes against *Vibrio parahaemolyticus*, *Aquaculture* **172** (1999) 205-222.

[21] N. Miyoshi, C. Shimizu, S. Miyoshi, and S. Shinoda, Purification and characterization of *Vibrio vulnificus* protease, *Microbiol. Immunol.* **31** (1987) 13-25.

[22] J. W. P. Teo, L.-H. Zhang, and C. L. Poh, Cloning and characterization of a metalloprotease from *Vibrio harveyi* strain AP6, *Gene* **303** (2003) 147-156.

[23] M. Delaporte, P. Soudant, J. Moal, C. Lambert, C. Quere, P. Miner, G. Choquet, C. Paillard, and J. Samain, Effect of a mono-specific algal diet on immune functions in two bivalve species-*Crassostrea gigas* and *Ruditapes philippinarum.*, *J. Exp. Biol.* **206** (2003) 3053-3064.

[24] C. Lambert, P. Soudant, G. Choquet, and C. Paillard, Measurement of *Crassostrea gigas* hemocyte oxidative metabolism by flow cytometry and the inhibiting capacity of pathogenic vibrios, *Fish Shellfish Immunol.* **15** (2003) 225-240.

[25] C. Montagnani, C. Kappler, J. M. Reichhart, and J. M. Escoubas, Cg-Rel, the first Rel/NF-kappaB homolog characterized in a mollusk, the Pacific oyster *Crassostrea gigas*, *FEBS Lett.* **561** (2004) 75-82.

[26] M. W. Pfaffl, A new mathematical model for relative quantification in real-time RT-PCR, *Nucleic Acids Res.* **29** (2001) 2002-2007.

[27] K. J. Livak, and T. D. Schmittgen, Analysis of relative gene expression data using real-time quantitative PCR and the 2(-Delta Delta C(T)) Method, *Methods* **25** (2001) 402-408.

[28] R. A. Elston, Infectious diseases of the Pacific oyster, *Crassostrea gigas*, *Annu. Rev. Fish Dis.* (1993) 259-276.

[29] T. Li, M. Ding, J. Zhang, J. Xiang, and R. Liu, Studies on the pustule disease of abalone (*Haliotis discus hannai* Ino) on the Dalian coast, *J. Shellfish Res.* **17** (1998) 707-711.

[30] A. Lacoste, F. Jalabert, S. Malham, A. Cueff, F. Gelebart, C. Cordevant, M. Lange, and S. Poulet, A *Vibrio splendidus* strain is associated with summer mortality of juvenile oysters *Crassostrea gigas* in the Bay of Morlaix (North Brittany, France). *Dis. Aquat. Organ.* **46** (2001) 139-145.

[31] C. S. Friedman, and R. P. Hedrick, Pacific oyster nocardiosis: Isolation of the bacterium and induction of laboratory infections, *J. Invertebr. Pathol.* **57** (1991) 109-120.

[32] M. Gay, T. Renault, A. M. Pons, and F. Le Roux, Two *Vibrio splendidus* related strains collaborate to kill *Crassostrea gigas*: taxonomy and host alterations., *Dis. Aquat. Organ.* **62** (2004) 65-74.

[33] C. S. Friedman, J. H. Beattie, R. A. Elston, and R. P. Hedrick, Investigation of the relationship between the presence of a Gram-positive bacterial infection and summer mortality of the Pacific oyster, *Crassostrea gigas* Thunberg, *Aquaculture* **94** (1991) 1-15.

[34] P. Soudant, C. Paillard, G. Choquet, C. Lambert, H. I. Reid, A. Marhic, L. Donaghy, and T. H. Birkbeck, Impact of season and rearing site on the physiological and immunological parameters of the Manila clam *Venerupis* (=*Tapes*, =*Ruditapes*) *philippinarum*, *Aquaculture* **229** (2004) 401-418.

[35] F.-L. E. Chu, Defense mechanisms of marine bivalves., In Recent Advances in Marine Biotechnology. Immunobiology and Pathology, (ed. M. Fingerman and R. Nagabhushanam). Enfield, NH, Plymouth, UK: Science Publishers. 5 (2000) 1-42.

[36] J. Travis, J. Potempa, and H. Maeda, Are bacterial proteinases pathogenic factors?, *Trends Microbiol.* **3** (1995) 405-407.

[37] J. Torreilles, M. C. Guerin, and P. Roch, Reactive oxygen species and defense mechanisms in marine bivalves, *C. R. Acad. Sci III.* **319** (1996) 209-218.

[38] L. Bramble, and R. S. Anderson, Modulation of *Crassostrea virginica* hemocyte reactive oxygen species production by *Listonella anguillarum, Dev. Comp. Immunol.* **21** (1997) 337-348.

[39] C. Lambert, and J.-L. Nicolas, Specific inhibition of chemiluminescent activity by pathogenic Vibrios in hemocytes of two marine bivalves : *Pecten maximus* and *Crassostrea gigas*, *J. Invertebr. Pathol.* **71** (1998) 53-63.

[40] F. R. DeLeo, Modulation of phagocyte apoptosis by bacterial pathogens, *Apoptosis* **9** (2004) 399-413.

[41] R. Blomgran, L. Zheng, and O. Stendahl, Uropathogenic *Escherichia coli* Triggers Oxygen-Dependent Apoptosis in Human Neutrophils through the Cooperative Effect of Type 1 Fimbriae and Lipopolysaccharide, *Infect. Immun.* **72** (2004) 4570-4578.

[42] P. Hofman, G. Le Negrate, B. Mograbi, V. Hofman, P. Brest, A. Alliana-Schmid, G. Flatau, P. Boquet, and B. Rossi, *Escherichia coli* cytotoxic necrotizing factor-1 (CNF-1) increases the adherence to epithelia and the oxidative burst of human polymorphonuclear leukocytes but decreases bacteria phagocytosis, *J. Leukoc. Biol.* **68** (2000) 522-528.

[43] M. D. Jacobson, and M. C. Raff, Programmed cell death and Bcl-2 protection in very low oxygen, *Nature* **374** (1995) 814-816.

[44] P. A. Sandstrom, P. W. Tebbey, S. Van Cleave, and T. M. Buttke, Lipid hydroperoxides induce apoptosis in T cells displaying a HIV-associated glutathione peroxidase deficiency, *J. Biol. Chem.* **269** (1994) 798-801.

[45] K. Terahara, K. G. Takahashi, and K. Mori, Pacific oyster hemocytes undergo apoptosis following cell-adhesion mediated by integrin-like molecules, *Comp. Biochem. Physiol. A Mol. Integr. Physiol.* **141** (2005) 215-222.

[46] I. Fridovich, Superoxide radical and superoxide dismutases, *Annu. Rev. Biochem.* **64** (1995) 97-112.

Figure legends

Fig. 1 Cumulative mortality (expressed in percentage) of *C. gigas* oysters non-injected (grey line) or injected either with *V. aestuarianus* 01/32 (black line) or with filtered sterile seawater (FSSW, dotted grey line). Asterisk (*) indicates significant difference between treatments within date (mean ± S.D.; N=4; ANOVA, P<0.05).

Fig. 2 (**A**) : Quantification of kanamycin-resistant *V. aestuarianus* 01/32 in filtered sterile seawater (control, dotted line) and in cell-free serum samples of *C. gigas* oysters following bacterial injection (black line). (**B**) : Reduced MTS/PMS absorbance as an estimation of the total bacterial load in control (dotted line) and in cell-free serum samples of *C. gigas* oysters after injection with *V. aestuarianus* 01/32 (black line), filtered sterile seawater (dotted grey line) or non-injected (grey line). Asterisk (*) indicates significant difference between treatments within date (mean ± S.D.; N=4; ANOVA, P < 0.05).

Fig. 3 (**A**) : Hemolymph total protease activity of *C. gigas* oysters collected 1-, 3-, 5- and 8 days after injection with *V. aestuarianus* 01/32 (black bars), filtered sterile seawater (grey bars) or non-injected (open bars). Asterisk (*) indicates significant difference between treatments within date (mean ± S.D.; N=4; ANOVA, P < 0.05). (**B**) : representative patterns of gelatinolytic activity in the hemolymph (4 - 5 µg protein/lane) of oysters after injection with *V. aestuarianus* 01/32 (**v**) or with filtered sterile seawater (**f**). Bands of protease activity are shown as clear bands over a dark background. "**ECP**" corresponds to the protease profile of crude *V. aestuarianus* 01/32 extracellular products, and "**M**" to the molecular weight marker.

Fig. 4 Total hemocyte counts (THC) of *C. gigas* oysters collected 1-, 3-, 5- and 8 days after injection with *V. aestuarianus* 01/32 (black line), filtered sterile seawater (dotted grey line) or non-injected (grey line). Asterisk (*) indicates significant differences between treatments within date (mean ± S.D.; N=4; Kruskal-Wallis, $P < 0.05$).

Fig. 5 Phagocytic activity of hemocytes (percentage of hemocytes containing 3 beads or more) measured in *C. gigas* oysters collected 1-, 3-, 5- and 8 days after injection with *V. aestuarianus* 01/32 (black bars), filtered sterile seawater (grey bars) or non-injected (open bars). Asterisk (*) indicates significant difference between treatments within date (mean ± S.D.; N=4; ANOVA, $P < 0.05$).

Fig. 6 Percentage of adherent hemocytes measured in *C. gigas* oysters collected 1-, 3-, 5- and 8 days after injection with *V. aestuarianus* 01/32 (black bars), filtered sterile seawater (grey bars) or non-injected (open bars). Asterisk (*) indicates significant difference between treatments within date (mean ± S.D.; N=4; ANOVA, $P < 0.05$).

Fig. 7 Mean ROS production level (DCF fluorescence in arbitrary unit A.U.), after 2-hours incubation in FSSW, of hemocytes from *C. gigas* oysters collected 1-, 3-, 5- and 8 days after injection with *V. aestuarianus* 01/32 (black line), filtered sterile seawater (dotted grey line) or non-injected (grey line). Asterisk (*) indicates significant differences between treatments within date (mean ± S.D.; N=4; Kruskal-Wallis, $P < 0.05$). (a) : granulocyte sub-population (b) : hyalinocyte sub-population.

Fig. 8 Relative expression of *Cg-EcSOD* and *Cg-TIMP* measured in oysters collected 1-, 3-, 5- and 8 days following injection with *V. aestuarianus* 01/32 (black bars) or with filtered

sterile seawater (grey bars). The error bars represent one standard deviation. Comparison of the level of mRNA (relative to *EF* mRNA) between fssw- and vibrio-conditions was performed by Student's t test; (*) significant at the 5% level.

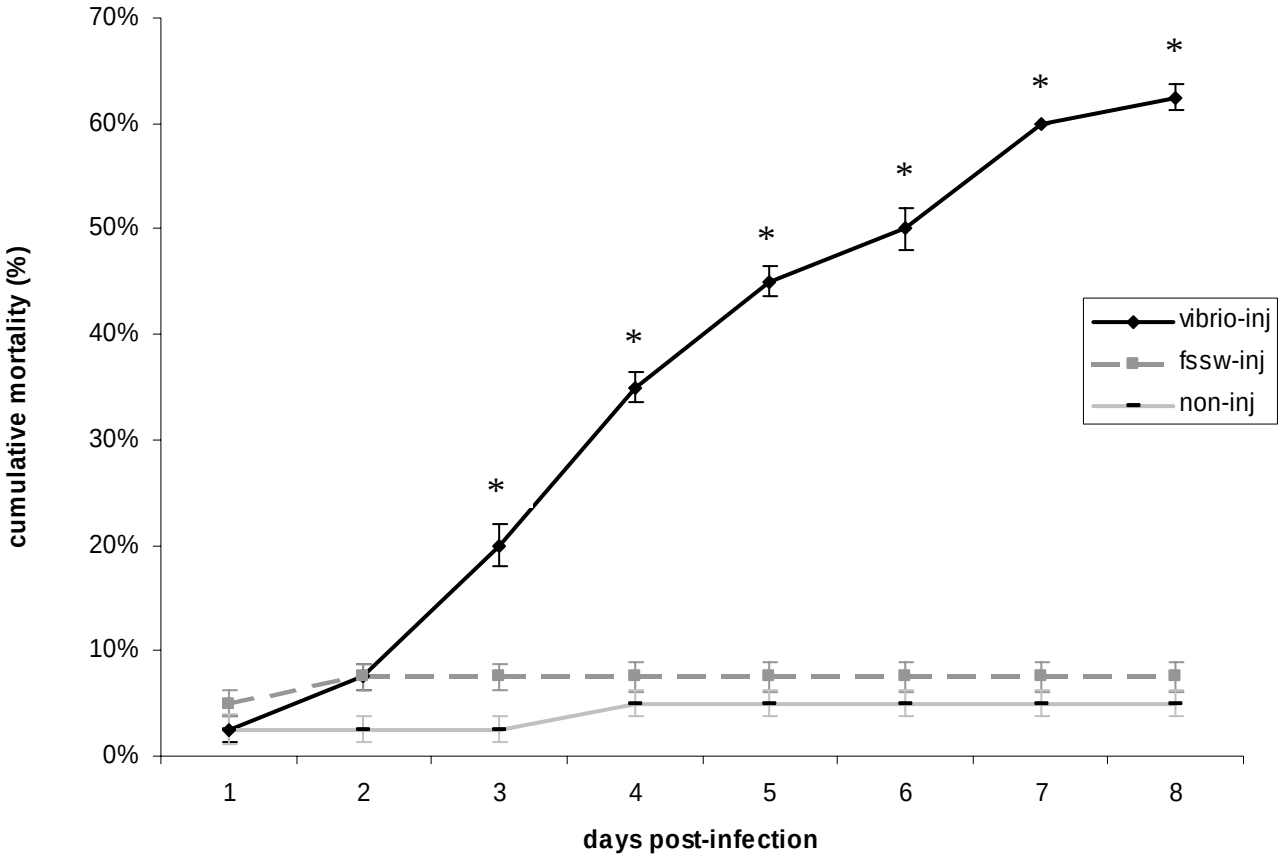
70%
60%
50%
40%
30%
20%
10%
0%
cumulative mortality (%)
1
2
3
4
5
6
7
8
days post-infection
vibrio-inj
fssw-inj
non-inj
*
*
*
*
*
*

Fig. 1

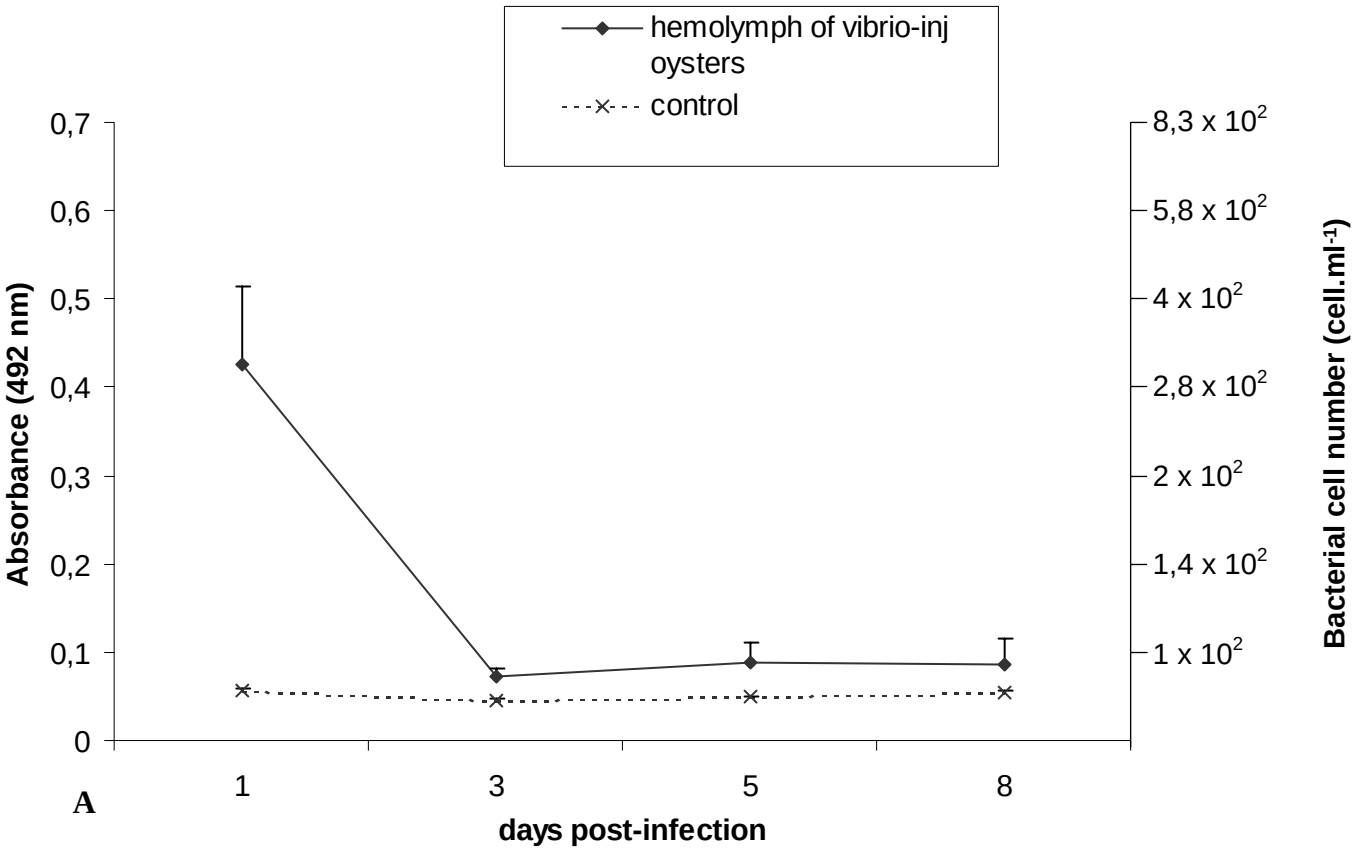
hemolymph of vibrio-inj oysters
control
Absorbance (492 nm)
Bacterial cell number (cell.ml-1)
0,7
0,6
0,5
0,4
0,3
0,2
0,1
0
8,3 x 10²
5,8 x 10²
4 x 10²
2,8 x 10²
2 x 10²
1,4 x 10²
1 x 10²
1
3
5
8
days post-infection
A

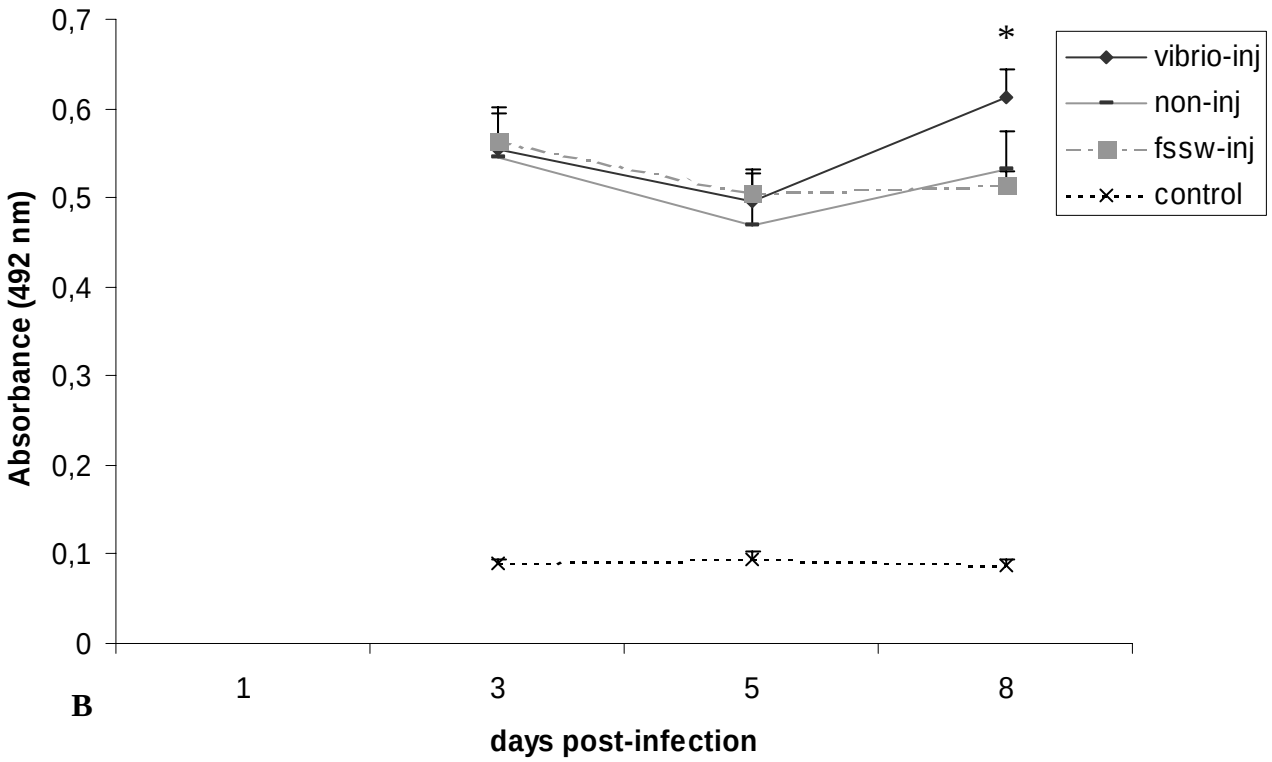
vibrio-inj
non-inj
fssw-inj
control
Absorbance (492 nm)
0,7
0,6
0,5
0,4
0,3
0,2
0,1
0
*
1
3
5
8
days post-infection
B

Fig. 2

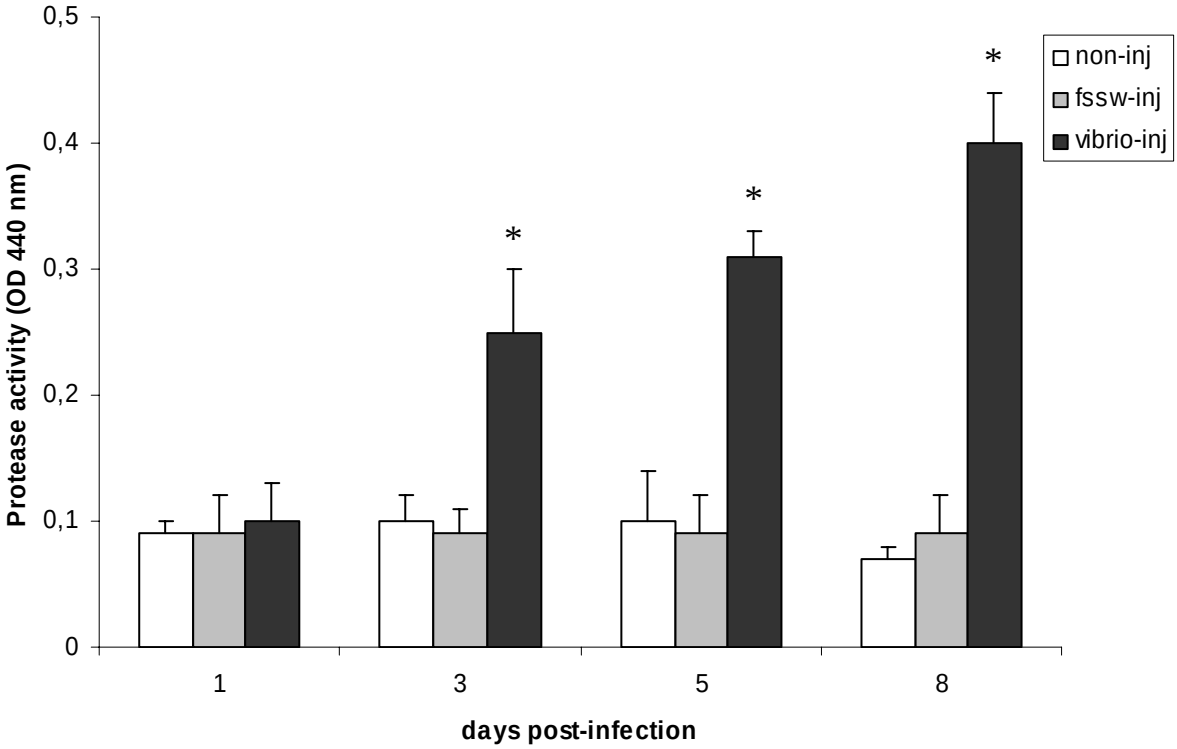
0,5
0,4
0,3
0,2
0,1
0
Protease activity (OD 440 nm)
non-inj
fssw-inj
vibrio-inj
*
*
*
1
3
5
8
days post-infection

A

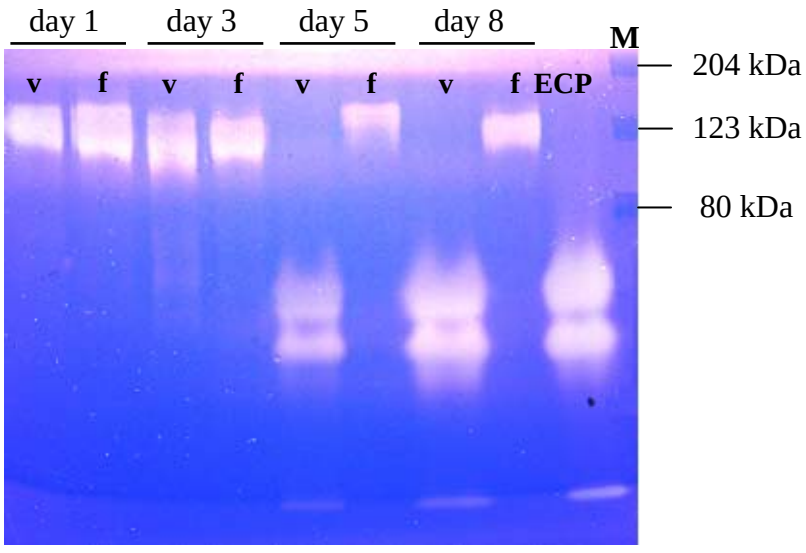
day 1
day 3
day 5
day 8
M
v
f
v
f
v
f
v
f
ECP
204 kDa
123 kDa
80 kDa

B

Fig. 3

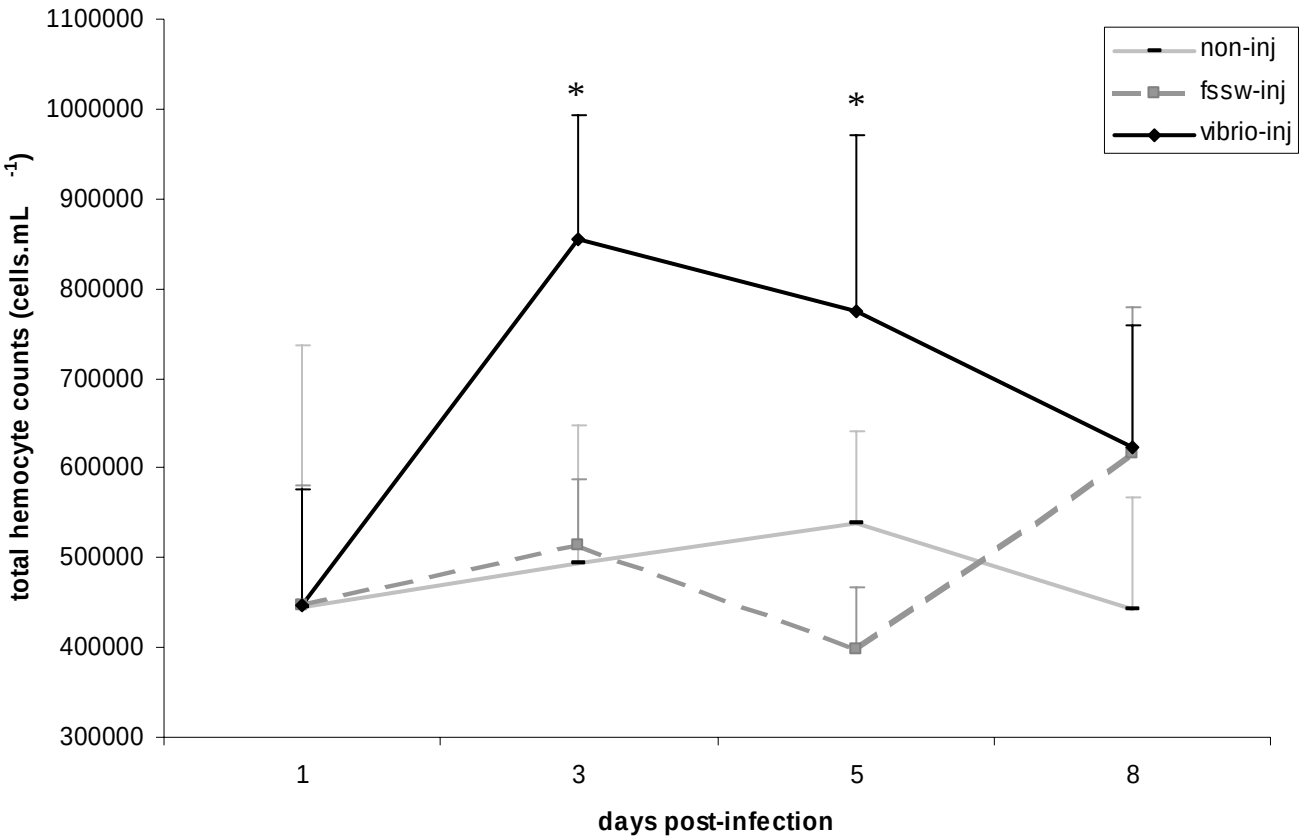
1100000
1000000
900000
800000
700000
600000
500000
400000
300000
total hemocyte counts (cells.mL -1)
1
3
5
8
days post-infection
*
*
non-inj
fssw-inj
vibrio-inj

Fig. 4

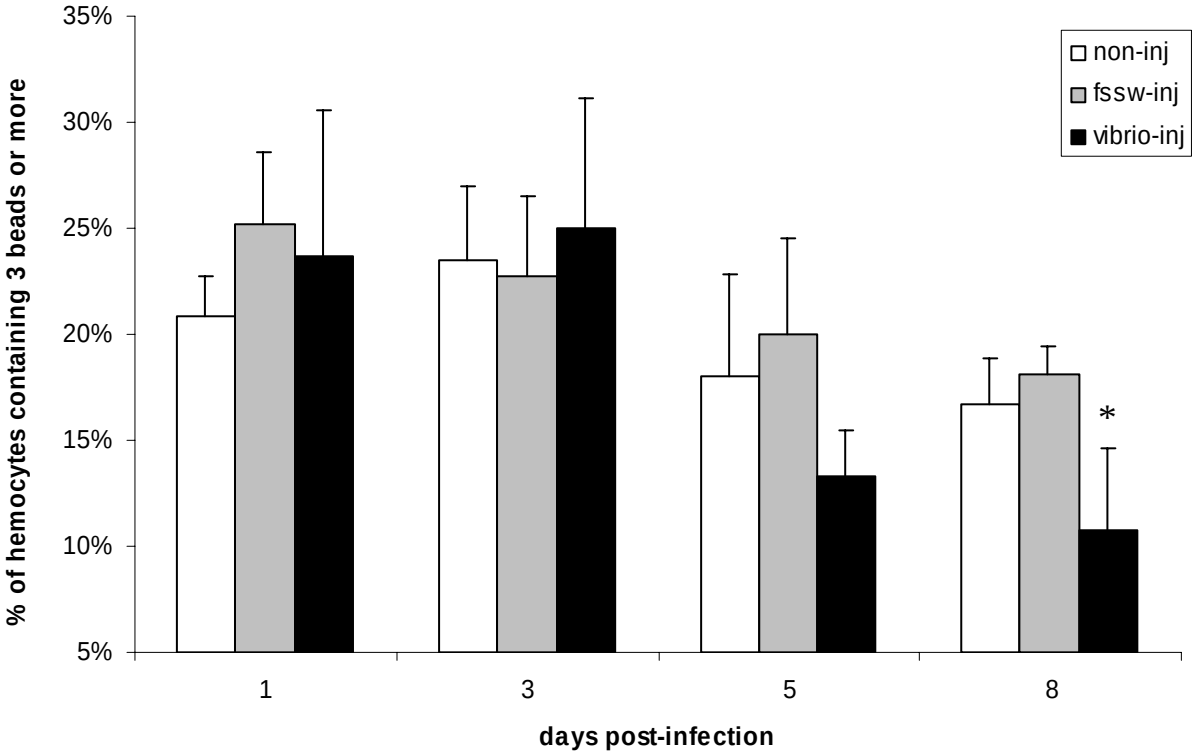
35%
30%
25%
20%
15%
10%
5%
% of hemocytes containing 3 beads or more
1
3
5
8
days post-infection
non-inj
fssw-inj
vibrio-inj
*

Fig. 5

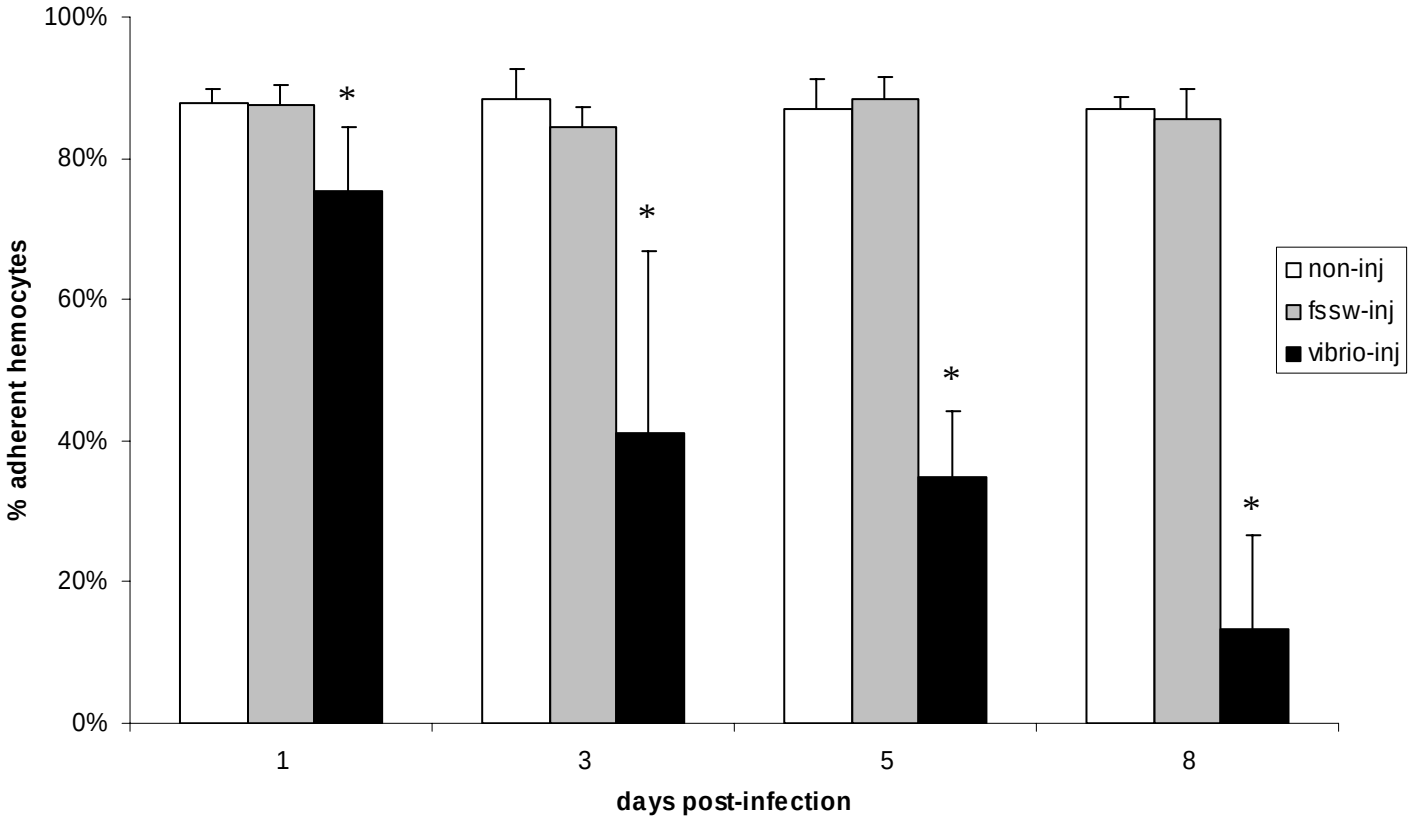
100%
80%
60%
40%
20%
0%
% adherent hemocytes
1
3
5
8
days post-infection
non-inj
fssw-inj
vibrio-inj
*
*
*
*

Fig. 6

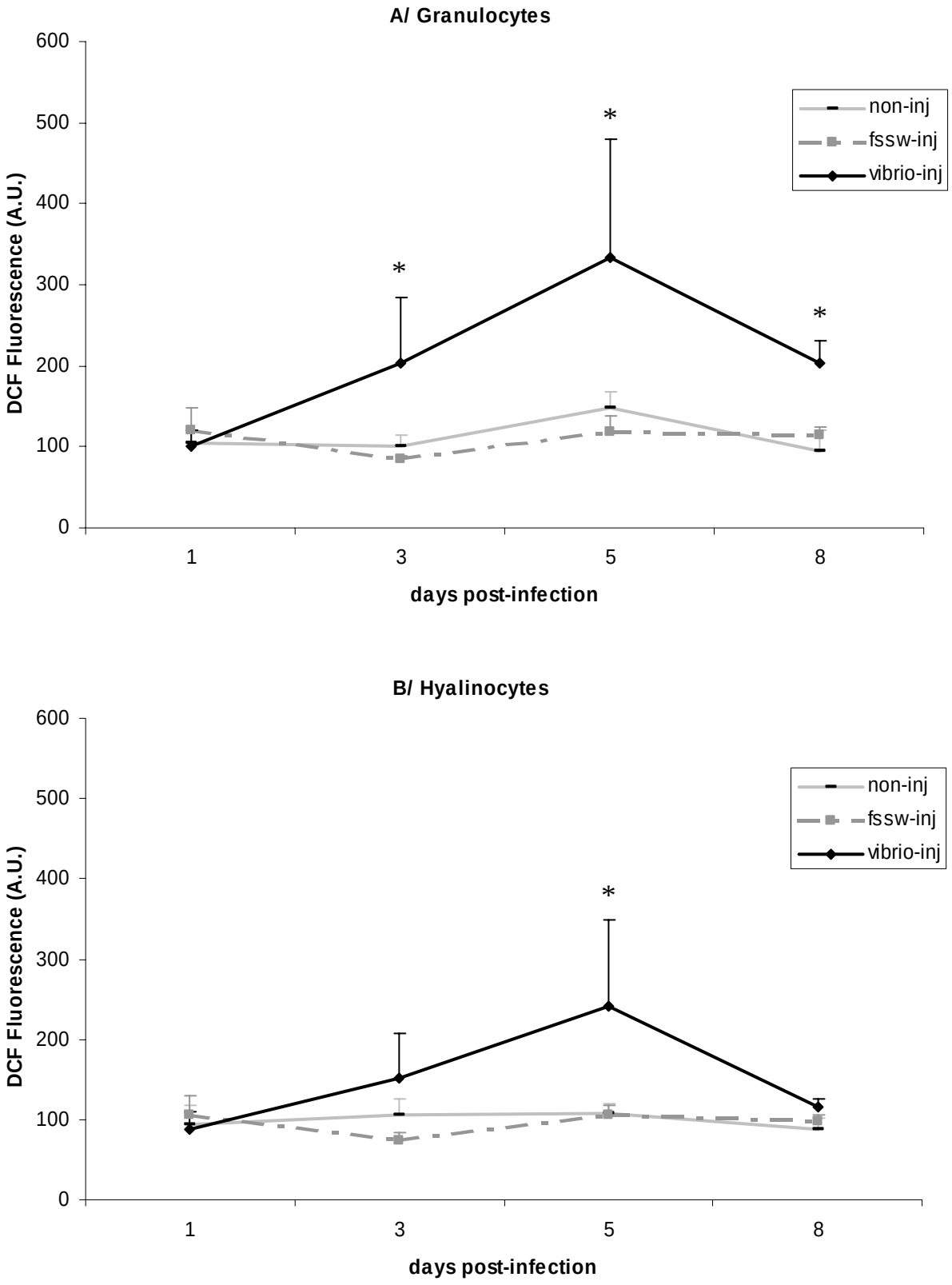
A/ Granulocytes
DCF Fluorescence (A.U.)
600
500
400
300
200
100
0
1
3
5
8
days post-infection
non-inj
fssw-inj
vibrio-inj
*
*
*
B/ Hyalinocytes
DCF Fluorescence (A.U.)
600
500
400
300
200
100
0
1
3
5
8
days post-infection
non-inj
fssw-inj
vibrio-inj
*

Fig. 7

A / ***Cg-EcSOD***

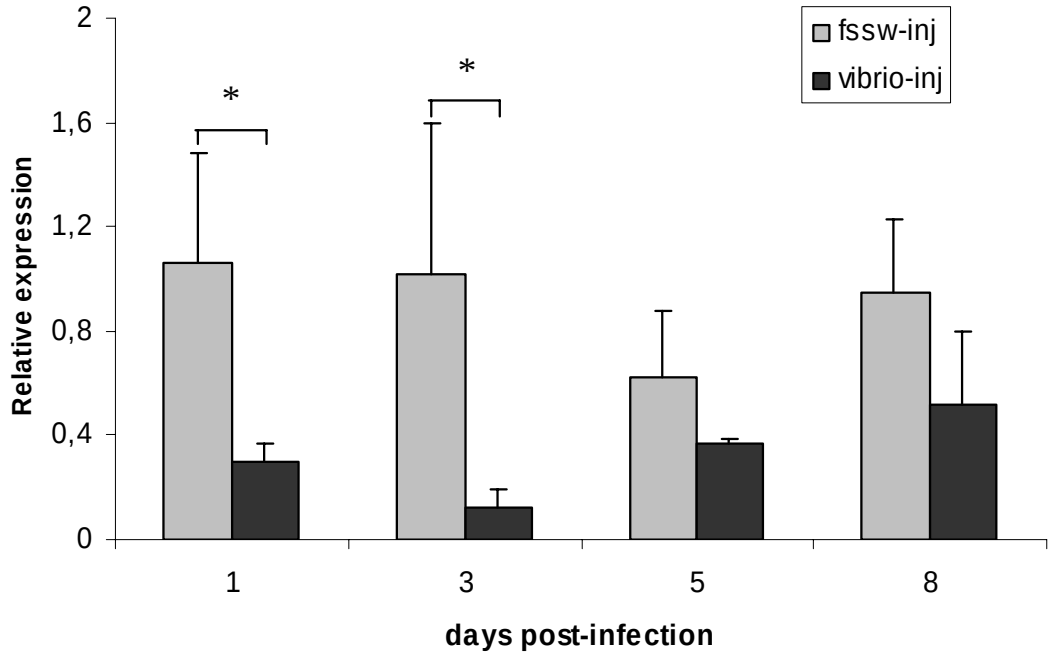

B/ ***Cg-TIMP***

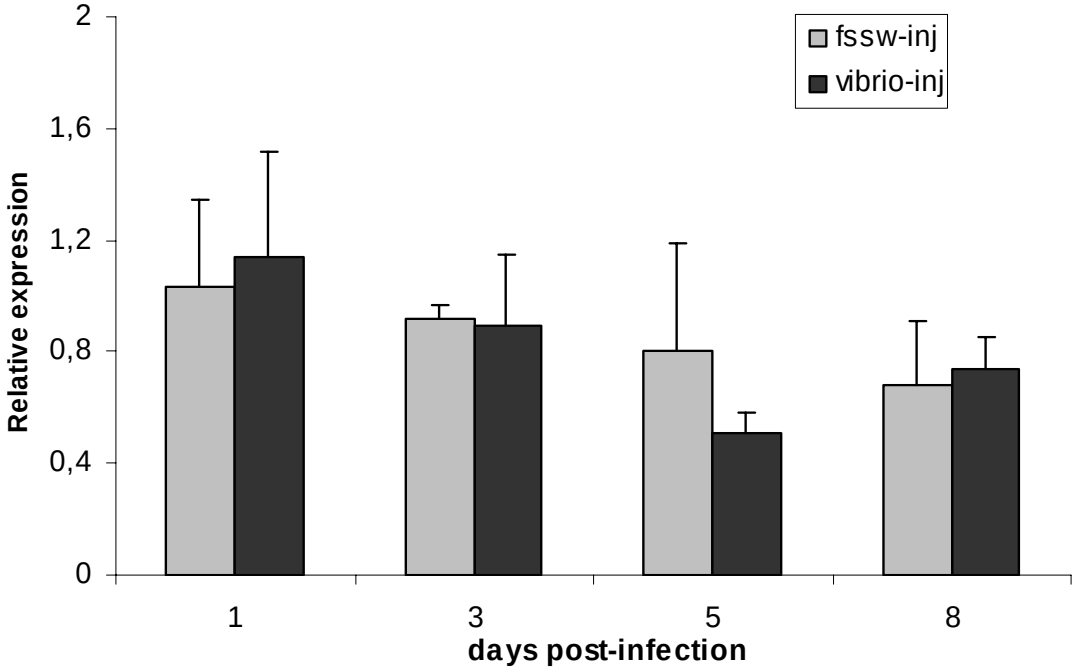

Fig. 8